

Improved Temperature Stability in Dielectric Properties of $0.8\text{BaTiO}_3\text{-(}0.2\text{-x)NaNbO}_3\text{-xBi(Mg}_{1/2}\text{Ti}_{1/2})\text{O}_3$ Relaxors

Yumin Goh*, Baek-Hyun Kim**, Hyunjeong Bae**, and Do-Kyun Kwon***†

*Department of Materials Engineering, Korea Aerospace University, Goyang 10540, Korea

**Materials Research Institute, Korea Aerospace University, Goyang 10540, Korea

(Received March 7, 2016; Revised March 14, 2016; Accepted March 15, 2016)

ABSTRACT

Ferroelectric relaxor ceramics with $\text{BaTiO}_3\text{-NaNbO}_3\text{-Bi(Mg}_{1/2}\text{Ti}_{1/2})\text{O}_3$ ternary compositions (BT-NN-BMT) have been prepared by sol-gel powder synthesis and consequent bulk ceramic processing. Through the modified chemical approach, fine and single-phase complex perovskite compositions were successfully obtained. Temperature and frequency dependent dielectric properties indicated typical relaxor characteristics of the BT-NN-BMT compositions. The ferroelectric–paraelectric phase transition became diffusive when NN and BMT were added to form BT based solid solutions. BMT additions to the BT-NN solid solutions affected the high temperature dielectric properties, which might be attributable to the compositional inhomogeneity of the complex perovskite and resulting weak dielectric coupling of the Bi-containing polar nanoregions (PNRs). The temperature stability of the dielectric properties was good enough to satisfy the X9R specification. The quasi-linear P - E response and the temperature-stable dielectric properties imply the high potential of this ceramic compound for use in high temperature capacitors.

Key words : Relaxor, High temperature capacitor, BT-NN-BMT, Perovskite, X9R

1. Introduction

The rapid growth of the field of Electric or Hybrid Electric Vehicles (EV or HEV) has resulted in a push for a performance improvement in passive electronic components. Ceramics with stable electrical properties at high temperatures of over 150°C offer opportunities for developing high temperature electric devices for applications in electronic control systems for EVs or HEVs. Especially for capacitors in such power electronics, dielectric ceramics that possess high-energy density, low loss, and good temperature stability are needed.¹⁻⁴⁾

The BaTiO_3 based dielectrics usually display remarkable nonlinearity of the dielectric constant as a function of temperature due to the presence of a series of phase transitions. This behavior limits applications at extended temperature range. Improvements in the high temperature dielectric properties of BaTiO_3 based ferroelectrics have been achieved by forming complex perovskite solid solutions with heterovalent cations. Solid solutions of BaTiO_3 with Bi-based oxides have been studied extensively because the ferroelectric transition temperatures of complex perovskite materials can be controlled by compositional methods, which can be used to engineer the temperature dependence of the dielectric properties.⁵⁻⁸⁾ Most of these complex perovskite materials were relaxor dielectrics with diffuse, frequency dependent dielectric peaks associated with interactions of polar

nanoregions (PNRs). Relaxor ferroelectrics exhibit high polarization, while remnant polarization remains at a low value. These properties result in a slim P - E hysteresis loop, which makes these materials promising candidates for use in energy storage ceramic capacitors.⁹⁻¹¹⁾ A lead-free relaxor composition, $\text{BaTiO}_3\text{-Bi(Mg,Ti)O}_3$ (BT-BMT), has been found to exhibit attractive properties, especially for high temperature capacitor applications. With an increase in the BMT content in solid solution, the tetragonal ferroelectric phase is transformed into a pseudocubic phase. The phase transition to pseudocubic symmetry of the BT-BMT systems can be attributed to the low tolerance factor of BMT. For compositions with appropriate BMT content, broadened dielectric peaks correlated to the relaxor phase transitions gradually transfer to a temperature independent permittivity plateau accompanying frequency dependent relaxation.^{12,13)} In addition to the bulk ceramic forms, thin film BT-BMT prepared by chemical solution deposition has also been found to display stable dielectric properties at temperatures up to 200°C , with high polarization and slim hysteresis; these properties result in a high energy density of 37 J/cm^3 at 1.9 MV/cm .¹⁴⁾

Though the BT-BMT relaxors, with largely temperature-stable dielectric permittivity at high temperature, are promising materials for high temperature applications, they undergo a frequency dependent drop in dielectric permittivity due to relaxational freezing of the dipoles at around room temperature. This phenomenon limits the application of these materials at low temperatures. Our previous study on the $\text{BaTiO}_3\text{-NaNbO}_3$ (BT-NN) relaxor system showed a possible solution that could extend the applicable temperatures to lower than -100°C by shifting the dielectric peaks to a lower range. For the composition, $0.8\text{BT-}0.2\text{NN}$, a fre-

†Corresponding author : Do-Kyun Kwon

E-mail : dkwon@kau.ac.kr

Tel : +82-2-300-0164 Fax : +82-2-3158-3770

quency dependent broad phase transition occurred over the range of temperatures from -150°C to room temperature.¹⁵⁾

In this study, we replaced parts of the NaNbO₃ in the BT-NN system with Bi(Mg,Ti)O₃ to form BT-NN-BMT solid solutions. Since the NN addition occurs early relaxor transitions at very low temperatures and the BMT addition tends to enhance the polarization at high temperatures, the co-doping of NN and BMT into BT is expected to further extend the temperature range in which the high dielectric polarization can be maintained. The phase formation, micro structure, and dielectric properties of the BT-NN-BMT solid solutions are extensively analyzed and discussed.

2. Experimental Procedures

Barium acetate ((CH₃COO)₂Ba, Sigma-Aldrich), titanium(IV) isopropoxide (Ti[OCH(CH₃)₂]₄, Sigma-Aldrich), sodium ethoxide (CH₃CH₂ONa, Sigma-Aldrich), niobium(V) ethoxide (Nb(OCH₂CH₃)₅, Sigma-Aldrich), bismuth(III) nitrate pentahydrate (Bi(NO₃)₃·5H₂O, Sigma-Aldrich) and magnesium acetate tetrahydrate ((CH₃COO)₂Mg·4H₂O, Sigma-Aldrich) were selected as starting materials to synthesize the complex perovskite compounds via sol-gel powder synthesis method. Based on their solubility, the starting materials were dissolved separately in two different solvents. Barium acetate, magnesium acetate, and bismuth nitrate pentahydrate were dissolved in glacial acetic acid and chelated by acetylacetone. Titanium isopropoxide, sodium ethoxide, and niobium ethoxide were dissolved in 2-methoxyethanol under nitrogen atmosphere. Those two solutions were mixed together and stabilized by adding Triethanolamine, which prevents the hydrolysis reaction of metal alkoxides.¹⁶⁾ The final, stabilized precursor solution was transformed into a gel and subsequently dried at 200°C for 24 h to obtain fine powders. The dry powders were calcined at 600°C for 1 h, then ball milled with zirconia media in anhydrous ethanol for 24 h. The fine powders were pressed into pellets and sintered at 1300°C for 2 h.

The phase formation and crystal structures of the solid solution samples were investigated using an X-ray diffractometer (XRD; Ultima IV, RIGAKU). The surface microstructures of the thermally-etched samples were analyzed using a field-emission scanning electron microscope (FE-SEM; JSM-7001F, JEOL Ltd.). For dielectric characterizations, silver electrodes were plated on both sides of the polished pellets by screen-printing method. The pellets were around 7 mm in diameter and 1 mm in thickness. The screen printed silver paste (SJA-52-540, Sung Jee Tech) was cured at 180°C for 1 h to form a metallic phase. Capacitance and dielectric loss were measured as functions of temperature in a range of -150 ~ 200°C and frequency in a range of 10² ~ 10⁶ Hz using an impedance analyzer (4284 LCR meter, Agilent Technologies Inc.) in a Delta Design 9023 environmental test chamber. For the high temperature dielectric measurements at temperatures up to 400°C, a cube furnace with electrical test setup was employed. The

P-E hysteresis curve was measured on a ferroelectric tester (Precision LC, Radiant Technologies) in the Delta Design 9023 environmental test chamber, which enables polarization measurements at different temperatures varying from -50°C to 200°C.

3. Results and Discussion

Figure 1 shows the X-ray diffraction patterns of the various 0.8BaTiO₃-(0.2-x)NaNbO₃-xBi(Mg_{1/2}Ti_{1/2})O₃ (x = 0.05 ~ 0.15) compositions. The diffraction patterns for all three compositions suggest a pure perovskite structure without any secondary phase. For the (200) peak located near 45° of 2-theta, no peak splitting was detected. Therefore, it seems that the XRD peaks of the BT-NN-BMT compositions can be indexed to a pseudocubic symmetry.^{17,18)} When we carefully checked the peak positions of the XRD patterns, no significant shift in peak positions could be observed with increasing BMT content, which substitute for NN in the solid solutions. This phenomenon indicates that the interplanar spacing of the perovskite structure does not change much when Bi³⁺, Mg²⁺, and Ti⁴⁺ replace Na⁺ and Nb⁵⁺ ions in the BT-NN solid solution. It is believed that the Mg²⁺ and Ti⁴⁺ ions were more likely to enter the B-site substituting Nb⁵⁺, and that Bi³⁺ ions were more likely to enter the A-site substituting Na⁺. For the complex perovskite with pseudocubic symmetry, it is believed that the B-O₆ octahedra dominate the unit cell volume. Since the mean B-site ionic radii of BMT ($\frac{1}{2}r(\text{Mg}^{2+}) + \frac{1}{2}r(\text{Ti}^{4+}) = 0.662\text{\AA}$) is very close to the size of the Nb⁵⁺ ion ($r = 0.64\text{\AA}$), it is reasonable to say that the BMT addition to the BT-NN would have a negligible effect on the lattice spacing.¹⁹⁾

Field emission scanning electron microscopy (FE-SEM) images of the thermally etched surfaces of the BT-NN-BMT ceramics, which were sintered at 1300°C for 2 h, are shown in Fig. 2. For the samples with small amounts of BMT addi-

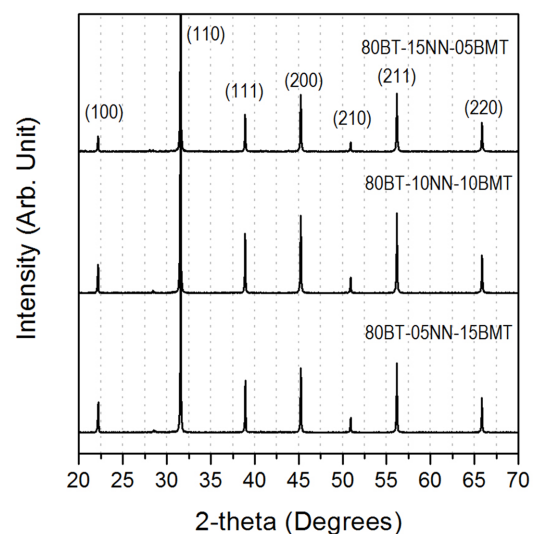


Fig. 1. Powder X-Ray diffraction patterns of 0.8BT-(0.2-x)NN-xBMT solid solutions.

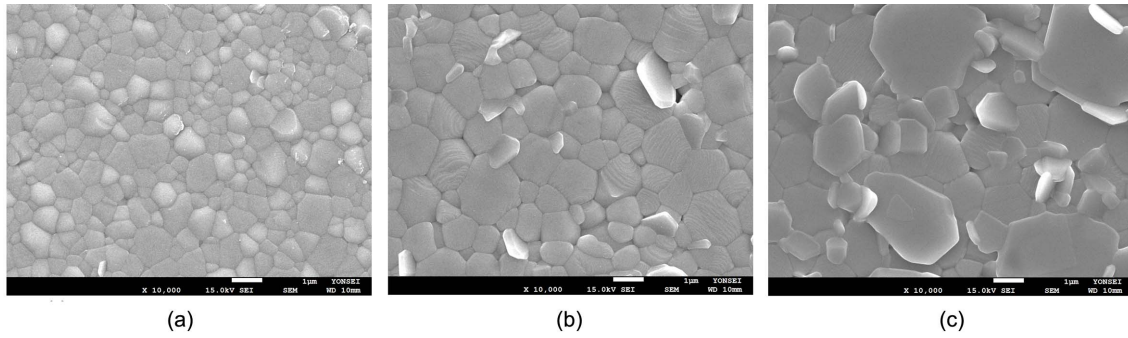


Fig. 2. Surface microstructures of 0.8BT-(0.2-x)NN-xBMT ceramics sintered at 1300°C for 2 h. (a) $x = 0.05$, (b) $x = 0.1$, and (c) $x = 0.15$.

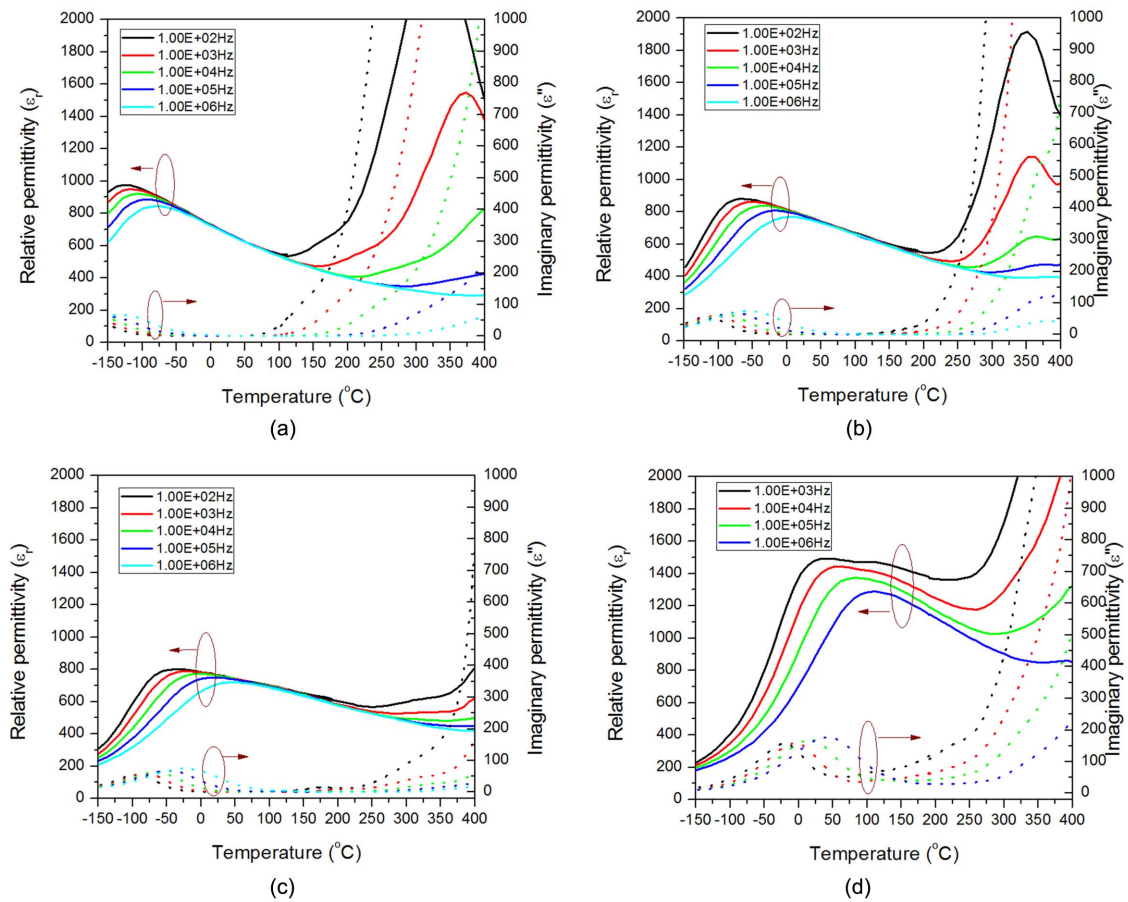


Fig. 3. Temperature and frequency dependent real and imaginary parts of dielectric permittivities for 0.8BT-(0.2-x)NN-xBMT ceramic samples with compositions of (a) $x = 0.05$, (b) $x = 0.10$, (c) $x = 0.15$, and (d) $x = 0.20$.

tion ($x = 0.05$), fine and dense microstructure with grains in sub-micron size was observed. However, significant grain growth and morphology change were observed with increasing BMT content. For $x = 0.1$, the grains became larger and plate shaped anisotropic grains started to be developed. Further BMT addition promoted in-plane directional grain growth, which resulted in a plate-like morphology of the microstructure. It has been reported that grains of layered perovskite materials are inclined to grow along a - b planes and to develop a plate-like morphology in the presence of

liquid phase at elevated temperatures. Therefore, the plate-like grain development can be attributed to anisotropic grain growth enhanced by the presence of low melting Bi-compounds.²⁰⁾

Figure 3 shows the temperature dependent dielectric permittivities (real and imaginary parts) of the 0.8BT-(0.2-x)NN-xBMT solid solutions measured at different frequencies upon cooling. The temperature range of the measurement was from 400°C to -150°C. For all the samples, diffuse, frequency-dependent permittivity maximum peaks

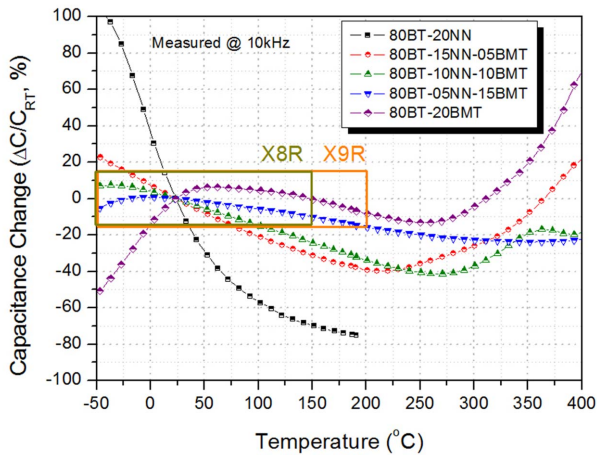


Fig. 4. Temperature dependent capacitance change of ceramic capacitors made of various $0.8\text{BT}-(0.2-x)\text{NN}-x\text{BMT}$ compositions.

upon transition, which are typical of relaxors, were observed. After the diffuse, frequency dependent phase transition, a relatively flat region in the dielectric permittivity change followed until there was another sharp increase in the dielectric constant and loss occurred. The sudden increases in dielectric constant and loss can generally be explained by a loss mechanism associated with ohmic conduction at high temperatures.¹⁸⁾ The temperature of the maximum dielectric constant (T_m) slightly increases with NN substitution by BMT. In addition, one obvious change in the temperature dependent dielectric permittivities with BMT addition was that the broadened phase transition peaks became a temperature stable permittivity plateau within the temperatures range of $-50^\circ\text{C} \sim 300^\circ\text{C}$ for the $x = 0.15$ composition. However, the temperature stable plateau range dropped again for samples with $x = 0.2$ compositions. It is known that compositional disorder and frustration are mainly responsible for producing relaxor characteristics because charge fluctuation consequently forms polar nanoregions (PNR).²¹⁾ Chemical disorder, which disturbs the Ti-O bond oscillations in the distorted oxygen octahedral frames, is generally accepted as being responsi-

ble for the diffuse, relaxor-type phase transitions that are represented by the broadening of the dielectric permittivity peak. It is also natural to assume that the development of the relaxor state in the hetero-substituted BT-based perovskite is closely related to random fields (RFs) arising due to the introduced charge disorder. For this reason, the relaxor state can be easily induced by a relatively low doping level in the case of hetero-valent substitutions at both the A- and B- sites of the perovskite structure. When two or more cations occupy the same crystallographic lattice site, the development of long range polar ordering is impeded.^{22,23)} In the case examined in this study, the introduction of Bi^{3+} , Mg^{2+} , and Ti^{4+} ions further increased the compositional inhomogeneity of the BT-NN perovskite. Because the three different heterovalent cations share both A- (Ba^{2+} , Na^+ , Bi^{3+}) and B-sites (Ti^{4+} , Nb^{5+} , Mg^{2+}), the charge disorder in the lattice is believed to be enhanced by adding BMT up to $x = 0.15$, in the $0.8\text{BT}-(0.2-x)\text{NN}-x\text{BMT}$ compositions. Therefore, it is reasonable to say that the highest compositional and charge complexities of $0.8\text{BT}-0.05\text{NN}-0.15\text{BMT}$ are responsible for the temperature-stable permittivity plateau. It is also beneficial to have Bi^{3+} ions to extend the plateau region at high temperatures. Lone pair electrons in the Bi^{3+} ions are considered to be the origin of the enhanced polarization response of the Bi-based perovskite materials.²⁴⁾ The existence of the lone pair repulsive force applied to other bonding schemes generally causes a distortion of the structure, which results in spontaneous polarizations that are sustainable at high temperatures. Fig. 4 provides direct comparisons of the temperature stability of the capacitance for ceramic capacitors made of $0.8\text{BT}-(0.2-x)\text{NN}-x\text{BMT}$ ceramics with BMT contents varying from 0 to 0.2. The capacitances were measured at 10 kHz as a function of the temperature, which ranged from -55°C to 400°C . It can be very clearly observed that the temperature stability of the capacitance is significantly improved by the addition of BMT to the BT-NN ceramics. For the composition of $0.8\text{BT}-0.1\text{NN}-0.1\text{BMT}$, the temperature coefficient of the capacitance (TCC) satisfies the temperature stability specifications for X8R and X9R capacitors, which state that the capacitance change should fit within

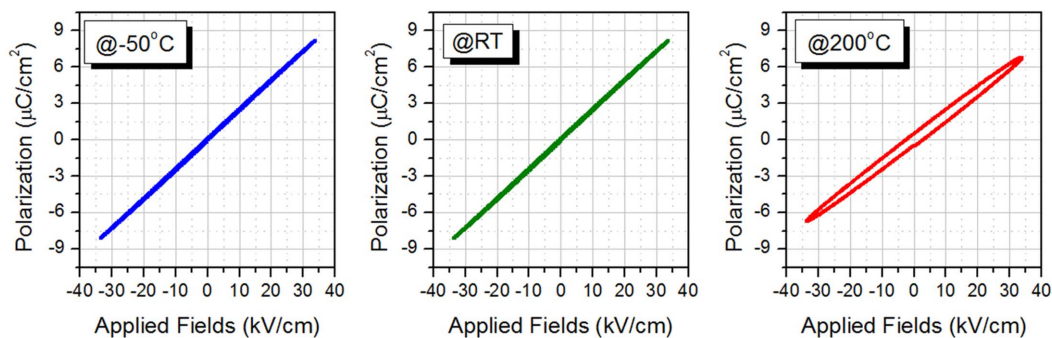


Fig. 5. Dielectric polarization response of the $0.8\text{BT}-0.05\text{NN}-0.15\text{BMT}$ ceramic samples against the applied electric field, measured at various temperatures.

$\pm 15\%$ of the tolerance limit for the temperature ranges of $-55^\circ\text{C} \sim 150^\circ\text{C}$ and $-55^\circ\text{C} \sim 200^\circ\text{C}$, respectively. The polarization responses against applied electric field for the 0.8BT-0.05NN-0.15BMT ceramics at different temperatures are found in Fig. 5. The polarization measurements for the ceramic samples were done under an applied electric field of ± 35 kV/cm. The linear (or quasi-linear) responses for the P - E plot, which indicates non-saturated typical relaxor behavior, were observed. The temperature dependence of the P - E response for the 0.8BT-0.05NN-0.15BMT ceramics can be explained using Fig. 3(c). The first-two measurement temperatures (-50°C and room temperature) correspond to the temperature regime for the relaxor transitions, especially for the cases of low-frequency measurements. It should be noted that the switching frequencies for the P - E measurement were in the range of 10 to 50 Hz. Because the dielectric constants at -50°C and at room temperature are close to each other (they lie on the plateau region), no big difference in P - E is expected. The quasi-linear P - E response was maintained at the elevated temperature of 200°C , though the polarization value decreased slightly due to the reduced dielectric constant at high temperatures. The increased loss tangent was also reflected in the P - E response, which exhibited hysteretic behavior at high temperature. The internal area of the P - E hysteresis loop corresponds to the amount of energy loss that occurred during the charge-discharge cycle.

4. Conclusions

Relaxor ferroelectric compositions, $0.8\text{BaTiO}_3-(0.2-x)\text{NaNbO}_3-x\text{Bi}(\text{Mg}_{1/2}\text{Ti}_{1/2})\text{O}_3$ solid solutions, have been fabricated by sol-gel powder synthesis followed by bulk ceramic sintering process. The solid solutions show a single-phase pseudocubic perovskite structure for all compositions. For all the 0.8BT-(0.2-x)NN-xBMT samples, diffuse, frequency-dependent permittivity maximum peaks upon transition, which are typical of relaxors, were observed. After the diffuse, frequency-dependent phase transition, a relatively flat region in the dielectric permittivity change followed until another sharp increase in the dielectric constant and the loss occurred. For the 0.8BT-(0.2-x)NN-xBMT ceramics, the temperature stability of the dielectric properties, which can be interpreted from the width of the temperature range in which the dielectric plateau is located in the ϵ - T plot, has been significantly improved by adding BMT to partially replace NN in 0.8BT-0.2NN solid solutions. Especially for the composition of 0.8BT-0.05NN-0.15BMT, the temperature coefficient of the capacitance (TCC) satisfies the temperature stability specifications for X9R capacitors. The excellent temperature stability of the dielectric properties means that this composition will be a good candidate for dielectric ceramic compositions for use in high temperature capacitor applications.

Acknowledgments

This research was supported by the Basic Science Research Program through the National Research Foundation of Korea (NRF), funded by the Ministry of Education (Grant #: NRF-2013R1A1A2061760)

REFERENCES

1. R. Dittmer, W. Jo, D. Damjanovic, and J. Rödel, "Lead-Free High-Temperature Dielectrics with Wide Operational Range," *J. Appl. Phys.*, **109** 034107 (2011).
2. Z. Liu, X. Chen, W. Peng, C. Xu, X. Dong, F. Cao, and G. Wang, "Temperature-Dependent Stability of Energy Storage Properties of $\text{Pb}_{0.97}\text{La}_{0.02}(\text{Zr}_{0.58}\text{Sn}_{0.335}\text{Ti}_{0.085})\text{O}_3$ Antiferroelectric Ceramics for Pulse Power Capacitors," *Appl. Phys. Lett.*, **106** [26] 262901 (2015).
3. H. Lee, J. R. Kim, M. Lanagan, S. Trolier-McKinstry, and C. A. Randall, "High-Energy Density Dielectrics and Capacitors for Elevated Temperatures: $\text{Ca}(\text{Zr,Ti})\text{O}_3$," *J. Am. Ceram. Soc.*, **96** [4] 1209-13 (2013).
4. D. P. Shay, N. J. Podraza, N. J. Bonnelly, and C. A. Randall, "High Energy Density, High Temperature Capacitors Utilizing Mn-Doped $0.8\text{CaTiO}_3-0.2\text{CaHfO}_3$ Ceramics," *J. Am. Ceram. Soc.*, **95** [4] 1348-55 (2012).
5. D. Tinberg and S. Trolier-McKinstry, "Structural and electrical Characterization of $x\text{BiScO}_3-(1-x)\text{BaTiO}_3$," *J. Appl. Phys.*, **101** [2] 4112 (2007).
6. H. Ogihara, C. Randall, and S. Trolier-McKinstry, "Weakly Coupled Relaxor Behavior of $\text{BaTiO}_3\text{-BiScO}_3$ Ceramics," *J. Am. Ceram. Soc.*, **92** [1] 110-18 (2009).
7. H. Ogihara, C. Randall, and S. Trolier-McKinstry, "High-Energy Density Capacitors Utilizing $0.7\text{BaTiO}_3-0.3\text{BiScO}_3$ Ceramics," *J. Am. Ceram. Soc.*, **92** [8] 1719-24 (2009).
8. C.-C. Huang and D. Cann, "Phase Transition and Dielectric Properties in $\text{Bi}(\text{Zn}_{1/2}\text{Ti}_{1/2})\text{O}_3\text{-BaTiO}_3$ Perovskite Solid Solutions," *J. Appl. Phys.*, **104** 024117 (2008).
9. Z. Yu, C. Ang, R. Guo, and A. S. Bhalla, "Ferroelectric-Relaxor Behavior of $\text{Ba}(\text{Ti}_{0.7}\text{Zr}_{0.3})\text{O}_3$ Ceramics," *J. Appl. Phys.*, **92** 2655-57 (2002).
10. A. Chen, Y. Zhi, and J. Zhi, "Impurity-Induced Ferroelectric Relaxor Behavior in Quantum Paraelectric SrTiO_3 and Ferroelectric BaTiO_3 ," *Phys. Rev. B*, **61** [2] 957 (2000).
11. J. Zhi, A. Chen, Y. Zhi, P. M. Vilarinho, and J. L. Baptista, "Dielectric Properties of $\text{Ba}(\text{Ti}_{1-y}\text{Y}_y)\text{O}_3$ Ceramics," *J. Appl. Phys.*, **84** 983-86 (1998).
12. D. H. Choi, A. Baker, M. Lanagan, S. Trolier-McKinstry, and C. Randall, "Structural and Dielectric Properties in $(1-x)\text{BaTiO}_3-x\text{Bi}(\text{Mg}_{1/2}\text{Ti}_{1/2})\text{O}_3$ Ceramics ($0.1 \leq x \leq 0.5$) and Potential for High-Voltage Multilayer Capacitors," *J. Am. Ceram. Soc.*, **96** [7] 2197-202 (2013).
13. Q. Zhang, Z. Li, F. Li, and Z. Xu, "Structural and Dielectric Properties of $\text{Bi}(\text{Mg}_{1/2}\text{Ti}_{1/2})\text{O}_3\text{-BaTiO}_3$ Lead-Free Ceramics," *J. Am. Ceram. Soc.*, **94** [12] 4335-39 (2011).
14. D.-K. Kwon and M. H. Lee, "Temperature-Stable High-Energy-Density Capacitors Using Complex Perovskite Thin Films," *IEEE Trans. Ultrason. Ferroelectrics Freq. Contr.*, **59** [9] 1894-99 (2012).
15. D.-K. Kwon, Y. Goh, D. Son, B. H. Kim, H. Bae, S. Perini,

- and M. Lanagan, "Temperature- and Frequency- Dependent Dielectric Properties of Sol-Gel-Derived BaTiO_3 - NaNbO_3 Solid Solutions," *J. Electron. Mater.*, **45** [1] 631-38 (2016).
16. C. E. Kim, Y. I. Park, and H. W. Lee, "Preparation of PbTiO_3 Fibres Using Triethanolamine-Complexed Alkoxide," *J. Mater. Sci. Lett.*, **16**, 96 (1997).
17. T. Wang, L. Jin, C. Li, Q. Hu, and X. Wei, "Relaxor Ferroelectric BaTiO_3 - $\text{Bi}(\text{Mg}_{2/3}\text{Nb}_{1/3})\text{O}_3$ Ceramics for Energy Storage Application," *J. Am. Ceram. Soc.*, **98** [2] 559-66 (2015).
18. A. Zeb and S. J. Milne, "Stability of High Temperature Dielectric Properties for $(1-x)\text{Ba}_{0.8}\text{Ca}_{0.2}\text{TiO}_3-x\text{Bi}(\text{Mg}_{0.5}\text{Ti}_{0.5})\text{O}_3$ Ceramics," *J. Am. Ceram. Soc.*, **96** [9] 2887-92 (2013).
19. R. Shannon, "Revised Effective Ionic Radii and Systematic Studies of Interatomic Distances in Halides and Chalcogenides," *Acta Crystallogr. Sect. A: Found. Crystallogr.*, **32** [5] 751-67 (1976).
20. C.-H. Lu and Y.-C. Chen, "Sintering and Decomposition of Ferroelectric Layered Perovskites: Strontium Dismuth Tantalate Ceramics," *J. Eur. Ceram. Soc.*, **19** [16] 2909-15 (1999).
21. J. Ravez and A. Simon, "Some Solid State Chemistry Aspects of Lead-Free Relaxor Ferroelectrics," *J. Solid State Chem.*, **162** [2] 260-65 (2001).
22. A. N. Salak, M. P. Seabra, and V. M. Ferreira, "Evolution from Ferroelectric to Relaxor Behavior in the $(1-x)\text{BaTiO}_3-x\text{La}(\text{Mg}_{1/2}\text{Ti}_{1/2})\text{O}_3$ System," *Ferroelectrics*, **318** [1] 185-92 (2005).
23. J. Wang, Y. Liu, K. Lau, R. L. Withers, Z. Li, and Z. Xu, "Dipolar-Glass-like Relaxor Ferroelectric Behavior in the $0.5\text{BaTiO}_3-0.5\text{Bi}(\text{Mg}_{1/2}\text{Ti}_{1/2})\text{O}_3$ Electroceramics," *Appl. Phys. Lett.*, **103** [4] 042910 (2013).
24. R. E. Cohen, "Origin of Ferroelectricity in Perovskite Oxides," *Nature*, **358** [6382] 136-38 (1992).